Acid-inducible proton influx currents in the plasma membrane of murine osteoclast-like cells

Miyuki Kuno, Guangshuai Li, Yoshie Moriura, Yoshiko Hino, Junko Kawawaki and Hiromu Sakai

Acid-inducible proton influx currents in the plasma membrane of murine osteoclast-like cells

Miyuki Kuno[1], Guangshuai Li[1], Yoshie Moriura[1], Yoshiko Hino[1], Junko Kawawaki[2], and Hiromu Sakai[1]

Department of Physiology[1] and Central Laboratory[2], Osaka City University Graduate School of Medicine, Abeno-ku, Osaka 545-8585, Japan.

Headings: Acid-inducible proton leak currents in osteoclasts

Please address correspondence to:
Dr. Miyuki Kuno
Department of Physiology
Osaka City University Graduate School of Medicine
1-4-3 Asahimachi, Abeno-ku, Osaka 545-8585
Tel: 81-06-6645-3711   Fax: 81-06-6645-3712
e-mail: kunomyk@med.osaka-cu.ac.jp

Abstract

Acidification of the resorption pits, which is essential for dissolving bone, is produced by secretion of protons through vacuolar H^+-ATPases in the plasma membrane of bone-resorbing cells, osteoclasts. Consequently osteoclasts face highly acidic extracellular environments, where the pH gradient across the plasma membrane could generate a force driving protons into the cells. Proton influx mechanisms during the acid exposure are largely unknown, however. In this study, we investigated extracellular acid-inducible proton influx currents in osteoclast-like cells derived from a macrophage cell line (RAW264). Decreasing extracellular pH to < 5.5 induced non-ohmic inward currents. The reversal potentials depended on the pH gradients across the membrane, and were independent of concentrations of Na^+, Cl^- and HCO_3^-, suggesting that they were carried largely by protons. The acid-inducible proton influx currents were not inhibited by amiloride, a widely-used blocker for cation channels/transporters, or by DIDS which blocks anion channels/transporters. Additionally, the currents were not significantly affected by V-ATPase inhibitors, bafilomycin A_1 and N,N'-dicyclohexylcarbodiimide. Extracellular Ca^{2+} (10 mM) did not affect the currents, but 1 mM $ZnCl_2$ decreased the currents partially. The intracellular pH in the vicinity of the plasma membrane was dropped by the acid-inducible H^+ influx currents, which caused overshoot of the voltage-gated H^+ channels after removal of acids. The H^+ influx currents were smaller in undifferentiated, mononuclear RAW cells and were negligible in COS7 cells. These data suggest that the acid-inducible H^+-influx (H^+-leak) pathway may be an additional mechanism modifying the pH environments of osteoclasts upon exposure to strong acids.

Key words: extracellular acidification, proton leak, proton influx current, osteoclast

Introduction

Osteoclasts dissolve bone tissue by acids and proteolytic enzymes which are secreted across the plasma membrane facing bone tissue (the ruffled membrane) into the resorption pit. As the ruffled membranes are rich in vacuolar-type H^+-ATPases (V-ATPase), osteoclasts could transfer protons uphill against the electrochemical gradient by using energy produced by ATP hydrolysis. The resorption pit is reported to be acidified to $6.8 - 4.7$ [23], and acidification is required to activate lysosomal enzymes (the optimum pH = $3 \sim 5$) and to degrade hydroxyapatite. Consequently, the ruffled membranes are exposed to extremely acidic extracellular environments. Under these conditions, the proton secretion through V-ATPases must decrease [18], and excess extracellular protons may enter the cells passively because of the large transmembrane concentration gradient for protons. However, the proton influx (proton-leak) mechanisms are largely unknown.

Some hints as to the mechanisms underlying the proton fluxes in response to the large pH gradients arise from the findings in intracellular acidic vesicles, such as phagosomes or lysosomes, the lumens of which are highly acidic (pH <5.5). In the steady state this is achieved by balancing the rates of proton pumping in by V-ATPases and passive proton leak [4, 24, 26]. Counter-ion conductances also contribute to the compensation of intravesicular charges generated by proton uptake. As the ruffled membranes are formed by exocytic fusion of lysosomes/endosomes [25], the two membranes may share common proton flux mechanisms, at least in part. It is known that the ruffled membranes possess V-ATPases and counter ion (Cl^-) conductances. However, passive proton leak mechanisms activated by acidification as strong as that of acidic vesicles have not been reported. If present, the "proton-leak" may be an additional mechanism which could modify the pH environments of osteoclasts.

This study investigated the extracellular acid-inducible H^+ influx pathways in plasma membranes exposed to highly acidic environments in osteoclast-like cells derived from RAW264 cells. We found that H^+ influx currents were activated by an extracellular pH (pH_o) lower than 5.5. The ambient pH might be

regulated by balancing transmembrane proton fluxes in opposite directions, the pumping out of H^+ and the proton influx. The present study provided evidence that the acid-inducible H^+ influx pathway was present in the plasma membrane of osteoclasts, suggesting that it may work as a passive H^+-leak mechanism when the extracellular space is highly acidified.

Materials and methods

Cells. Osteoclasts were generated from a mouse macrophage cell line (RAW264 cells) (Riken Cell Bank, Tsukuba, Japan) in the presence of a soluble form of receptor activator of nuclear factor κB ligand (sRANKL) (Peprotec EC Ltd; R & D), as described before [18-20]. RAW264 cells were maintained in the Dulbecco's modified MEM containing 100 U ml^{-1} penicillin, 0.1 mg ml^{-1} streptomycin, and 10% FCS at 37°C in a 95% air-5% CO_2 atmosphere. Treatment with 10-50 ng ml^{-1} of sRANKL in α-MEM with 5-10% FCS induced differentiation of RAW264 cells into multinucleated cells. One half of the medium was changed every two or three days. Osteoclast-like cells, identified by phase-contrast microscopy and TRAP (tartate-resistant acid phosphate) activity, appeared within 4 days and were maintained for 5-16 days. Recordings were made from cells containing ≥ 3 nuclei. The electrophysiological properties of the plasma membrane V-ATPases and voltage-gated H$^+$ channels in the RAW-derived osteoclasts share features with those in murine osteoclasts developed in primary culture [14-15, 18-20]. Some recordings were made in undifferentiated, mononuclear RAW cells, which were maintained in Dulbecco's modified MEM in the absence of sRANKL.

COS7 cells were maintained in Dulbecco's modified MEM and were used to compare the results with osteoclasts. COS7 cells lack native voltage-gated H$^+$ channels. To measure extracellular acid-induced changes in intracellular pH, as in osteoclasts, COS7 cells were transfected with a bicistronic vectors carrying cDNAs for a murine H$^+$ channel (Hv1/mVSOP) and green fluorescent protein (GFP) (kindly given by Y. Okamura) by lipofectamine LTX (Invitrogen). Transformed cells (COS/Hv cells) were identified by the expression of GFP. Electrical recordings were made from GFP-positive cells 36 - 72 hrs after the transfection. H$^+$ channel currents were recorded in all these GFP-positive cells.

Electrophysiological recordings. Whole cell recordings were made as described elsewhere [14, 18-20]. Current and voltage signals were recorded with an amplifier (Axopatch 200A, Axon Instruments, Foster City, CA, USA), digitized at 4 kHz with an analog-digital converter (Digidata 1200, Axon

Instruments) and analyzed using pCLAMP software (Axon Instruments). The reference electrode was a

Ag-AgCl wire connected to the bath solution through a saline-agar bridge. The pipette resistances were

5-15 MΩ.

For separating H^+ currents, the major cations and anions (K^+, Na^+ and Cl^-) in pipette and bath

solutions were replaced by NMDG and aspartate, unless stated otherwise. The pipette solutions contained

(in mM): 1) 120 MES, 65 NMDG-aspartate, 5 $MgCl_2$, 1 BAPTA (pH 5.5), 2) 100 HEPES, 90

NMDG-aspartate, 5 $MgCl_2$, 1 BAPTA (pH 6.5), and 3) 100 HEPES, 75 NMDG-aspartate, 5 $MgCl_2$, and 1

EGTA (pH 7.0 - 7.3). Na_2ATP (5 mM) was added into the pipette solutions immediately before use. The

extracellular solutions contained (in mM): 1) 100 HEPES, 75-90 NMDG-aspartate, 1 $CaCl_2$, 1 $MgCl_2$ (pH

7.3 - 6.5), 2) 100 MES, 75-90 NMDG-aspartate, 1 $CaCl_2$, 1 $MgCl_2$ (pH 6.0 – 5.0), and 3) 100 MES, 80-90

NMDG, 90-95 aspartate, 1 $CaCl_2$, 1 $MgCl_2$, 10 Cs-methanesulfonate (pH 4.8 – 4.0). The pH's were

adjusted by CsOH: final concentrations of Cs^+ were > 10 mM. Unless stated otherwise, bath solutions

contained 10 mM glucose and 50-100 μM of 4,4'-diisothiocyanato-2,2'-stilbenesulfonate (DIDS), a

blocker for Cl^-/anion transport: the Cl^- channels expressed in osteoclasts were inhibited by DIDS [7,

21-22]. Bovine serum albumin (BSA) (0.1%) was applied in early experiments, but was removed in later

experiments. The results were not affected by the presence of BSA. Most of the currents recorded under

these conditions are carried by protons [14, 18-20]. In some experiments, NMDG-aspartate was replaced

by tetramethylammonium (TMA)-methanesulfonate, Na-aspartate (50 mM) or $NaHCO_3$ (10 mM). In the

presence of Na^+, 50-100 μM amiloride was added to block Na^+-H^+ exchangers when the pH of pipette

solution was low (pH_p 5.5). The extracellular and intracellular Cl^- concentrations were 4 and 10 mM

unless stated otherwise. To change the Cl^- concentrations, NMDG-aspartate was replaced by NMDG-Cl.

The Cl^--free pipette solutions were prepared by replacing $MgCl_2$ by $MgSO_4$. The liquid junction

potentials were examined at the start and the end of the all recordings: the changes in the liquid junction

potentials during recordings lasting 45 – 70 min were 8 ± 3 mV (n = 15) with the nominally Cl^--free

6

pipette solutions, not significantly different from those with the solutions containing 10 mM Cl⁻ (4 ± 5 mV, n = 12), with the same reference electrode. The osmolarities of all solutions were 280 – 295 mosmol.

Voltage-steps or voltage-ramps (from -100 to 100 mV or from -100 to 150 mV: 200-250 mV s^{-1}) were applied at holding potentials of 0 to -80 mV every 10-20 seconds. Capacitive currents upon voltage changes were monitored by applying voltage steps (0 mV for 200 ms) preceding each voltage ramp and the offset currents during voltage ramps (C_m x dV/dt) were corrected. The whole-cell capacitance (C_m) was 165 ± 6 pF (n = 239). The capacitive currents generally terminated within 50 ms, which corresponded to the range between -100 and -90 mV of voltage ramps. Current amplitudes were measured after the termination of the capacitive currents. The slopes of the I-V relations for 0-50 mV and -90 - -50 mV (Slope$_{0-50}$ and Slope$_{-90 - -50}$) were obtained from linear fits: the latter voltage range was adjusted to exclude contamination of capacitive currents in cases where they lasted for >50 ms. The background leak currents were not subtracted, as they were not identified in each trace. To exclude background currents, we analyzed acid-inducible currents as the differences between before and after activation. The presence of the acid-inducible currents was detected sensitively by the changes in the slopes or the slope ratios (Slope$_{-90 - -50}$/Slope$_{0-50}$) (Fig. 1c). The slope ratio was also useful in monitoring the appearance of the late currents with linear I-V relationships. Cells were exposed to acidic solutions by perfusing the recording chamber (volume, ~0.8 ml) at a rate of about 1 ml min^{-1}. The bath solutions were replaced almost completely within ~ 1 min. All experiments were conducted at room temperature (22-26°C).

The nominal transmembrane pH gradients were obtained as the differences between the pH's of the extracellular solutions (pH$_o$) and the pipette solutions (pH$_p$). Changes in the intracellular pH (pH$_i$) during exposure to acid were estimated from the reversal potentials (V$_{rev-Hv}$) of the voltage-gated H$^+$ channels present in the plasma membranes. The V$_{rev-Hv}$'s were obtained by two methods, one from the tail current method and the other from current measurements at two different voltages [5, 10]. In the former, tail currents were recorded at different voltages following 1-2 s long prepotentials (40 - 120 mV). Leak

currents at each voltage, estimated with short (20 ms) depolarization pulses which could not activate H^+

channels, were subtracted. The V_{rev-Hv}'s were estimated as the zero-current potentials for the I-V

relationships of the corrected tail currents. In the latter method, the V_{rev-Hv}'s were estimated from the

current amplitudes at two different potentials: H^+ currents measured at the end of depolarization pulses

(80 - 140 mV for 0.5 – 4 s) and the tail currents at repolarization (-80 - 0 mV) were used. The voltages

and the durations were adjusted to the pH gradients across the membrane in each experimental condition.

Dissolution of hydroxyapatite. Hydroxyapatite particles (apamicron) were suspended in Ringer

solution (0.1 -0.5 mg ml^{-1}). Absorbance of the suspensions, which were stirred continuously, was

measured at 550 nm with the spectrophotometer in triplicate for each preparation (UV3100RL, Shimadzu,

Kyoto, Japan).

Statistics. Data were expressed as means ± s.e.m. The statistical significances ($p < 0.05$) were

evaluated using the unpaired Student's *t*-test.

Substances. MES and BAPTA were purchased from Dojindo Laboratories (Kumamoto, Japan)

and bafilomycin A_1 from Apollo Scientific (Cheshire, UK). Hydroxyapatite (apamicron) was kindly given

by Sekisui Chemical Co. Ltd (Osaka, Japan). All other chemicals were obtained from Sigma (St. Louis,

MO, USA) unless specified otherwise. A concentrated stock solution of Na_2ATP was prepared in 1 M

Tris-Cl. DIDS, and bafilomycin A_1 were dissolved in DMSO, N,N'-dicyclohexylcarbodiimide (DCCD) in

dichloromethane, and amiloride in distilled water. The final concentrations of DMSO and

dichloromethane were < 0.1%, which did not affect the results.

Results

Extracellular acid-induced changes in proton currents in osteoclasts

First, we examined changes of the H^+ currents following extracellular acidification. When Na^+, K^+ and Cl^- were replaced by $NMDG^+$ and aspartate$^-$, major contributors to the plasma membrane proton currents in osteoclasts are the V-ATPases [18, 20] and the voltage-gated H^+ channels [14-15, 19]. Both H^+ currents are generally outward, and are identified by their distinct electrophysiological and pharmacological properties. The current-voltage (I-V) relationships obtained by voltage ramps applied at a holding potential (-80 mV) were a mixture of these H^+ currents. With an acidic pipette solution (pH_p 5.5), the outward H^+ currents were prominent at pH_o 7.3 (Fig. 1a) [14, 18]: the linear currents at <50 mV were mediated mostly by V-ATPases and, the outwardly rectifying currents at large depolarization, mostly by the H^+ channels. These outward H^+ currents were decreased by acidifying the extracellular medium and vanished at pH_o ~5. Further acidification (pH_o 4) increased inward currents. With more alkaline pipette solutions (pH_p 7.3), the outward H^+ currents, particularly the H^+ channel currents, were small at pH_o 7.3 (Fig. 1b). Lowering pH_o to 5.5 decreased these outward currents, and exposure to pH_o 4.5 increased the inward currents.

The time courses of the changes in the current amplitudes at different voltages (-80, 0 and +80 mV) showed that, following the reductions in the outward currents at pH_o 5.5, the inward currents appeared after exposure to pH_o 4.5 (Fig 1c, top). The slopes of the I-V relationships calculated for two voltage ranges, 0-50 mV (middle, closed squares; S_{0-50}) and -90 - -50 mV (open squares; $S_{-90 - -50}$) were slightly decreased during exposure to pH_o 5.5, due to decreases in the outward currents. After exposure to pH_o 4.5, the slopes increased with the appearance of the inward currents. It is noteworthy that the slope ratios ($S_{-90 - -50}/S_{0-50}$) also increased sharply with activation of the inward currents (Fig. 1c, bottom), indicating that the acid-induced currents were inwardly rectified. The acid-induced inward currents were also observed in the presence of 200 μM DCCD, a non-specific proton pump inhibitor, which blocked the plasma

9

membrane V-ATPase currents in osteoclasts completely [18] (Fig. 1d): the cell was exposed to pH_o 4.4 three times (pH_p 7.0). The acid-induced inward currents were reversible and were activated repeatedly.

Thus strong extracellular acidification activated inward currents over a wide range of pH_p (5.5 - 7.3). The currents recorded by applying depolarizing voltage-steps at a holding potential of -80 mV showed the reduction of the outward currents and the appearance of the inward currents by exposure to acid (Fig. 2a with pH_p 5.5 and Fig. 2b with pH_p 7.3). The inward currents were also recorded by applying hyperpolarizing voltage-steps at a holding potential of 0 mV (Fig. 2c with pH_p 6.5). These acid-induced inward currents did not display time-dependent kinetics following either depolarization or hyperpolarization.

The acid-inducible inward currents were seldom observed at $pH_o \geq 6.0$. At pH_o 5.5, the acid-inducible currents were present in ~20% of cells with pH_p 7.3 (n = 14) but were negligible with pH_p 5.5 (n = 23). At pH_o 4.5, the inward currents were found in 90% (17/19) of cells with pH_p 7.3, 94% (17/18) with pH_p 6.5 and 89% (8/9) with pH_p 5.5. The amplitudes of the inward currents were measured under different pH_p's at two potentials, -80 and 0 mV: the former fell on the part of the IV relationships representing the slope range, $S_{-90 - -50}$, and the latter, on the part of S_{0-50}. The mean current-densities at -80 and 0 mV, normalized by the cell capacitance, were increased by decreasing pH_o (Fig. 2d). At both voltages, the inward currents appeared at pH_o lower than ~5.5 over a wide range of pH_p's from 5.5 to 7.3, suggesting that the pH_o, and not the pH gradient, was essential for activating the inward currents. The inward currents appeared when the pH_o was lowered than ~5.5.

In some cells, the inward currents were followed by increases of currents in both inward and outward directions during prolonged (> 5-10 min) exposure to $pH_o \leq 4.5$, particularly in recordings with higher pH_p (>7.0). These late currents had linear I-V relationships and were partially reversible after washout. In the present study, we focused on the early response, which will be designated hereafter as the acid-inducible inward current.

Acid-inducible inward currents were mediated by protons.

The V_{rev}'s of the acid-inducible influx currents were obtained from the intersections of the I-V

relationships before and after activation of the acid-inducible inward currents (Fig. 3a-b). The activation

was confirmed from the changes in the slopes of the I-V curves. Large depolarizations, however, often

destabilized recordings or activated outwardly-rectifying currents. In these cells, the slopes of the I-V

relationships at greater than 50 mV behave differently from S_{0-50} and $S_{-90 - -50}$ (data not shown), suggesting

that at large depolarizations the acid-inducible influx currents might be contaminated with the other

current, possibly the acid-sensing, outwardly rectifying Cl^- channels [7]. As the inhibition of the Cl^-

channels by 100 μM DIDS was incomplete at high voltages under pH_o 4.5 (by 93 ± 3% at 100 mV, n = 4),

the data with significant contamination of the outwardly rectifying currents were excluded from the

estimation of the V_{rev}. The measured V_{rev} values were dependent on both pH_o and pH_p, and were close to

the equilibrium potentials for H^+ (E_H) calculated from the Nernst equation for each pH_o/pH_p (dashed

lines) (Fig. 3c). The V_{rev}'s were not significantly affected by DCCD, a proton pump inhibitor: 71 ± 5 mV

(n = 6) at pH_o/pH_p 4.4/5.5 with DCCD and 64 ± 5 mV (n = 4) without DCCD. The equilibrium potentials

for $NMDG^+$ and aspartate$^-$ were -10 - + 10 mV and those for Cl^- were 23 mV for all combinations of

pH_o/pH_p.

Similar acid-inducible inward currents were observed in the presence of Na^+: the currents were

measured in the presence of 100 μM amiloride, a blocker of the Na^+-H^+ exchanger which could be

activated at low intracellular pH. When both extracellular and intracellular solutions contained 50 mM

Na^+, the V_{rev}'s were measured from the intersections of the I-V relationships before and after activation of

the acid-inducible inward currents (Fig. 3d). The V_{rev} was 76 ± 6 mV (n= 3) under pH_o/pH_p 4.5/5.5, which

is far from E_{Na} (0 mV), and were not affected significantly by the transmembrane concentration gradients

for Na^+ (Fig. 3e). The solutions were nominally free of HCO_3^-. An addition of 10 mM HCO_3^- into both

extracellular and intracellular solutions did not change the V_{rev}'s (Fig. 3e, rightmost). These data

suggested that the acid-inducible inward currents were mediated mainly by H^+.

To investigate the effects of other ions on the amplitudes of the acid-inducible inward currents, the

current-densities activated by exposures to pH_o 4.5 were measured at two potentials, 0 and -80 mV (Fig.

4). The acid-inducible influx currents were not affected by different combinations of extracellular and

intracellular Cl^- concentrations, and also by the presence of Na^+ (50 mM) or HCO_3^- (10 mM) in both

solutions (pH_p 7.3) (Fig. 4a). Major ions in the solutions, NMDG-aspartate, were weak bases and weak

acids, which might affect the results through their proton-shuttle effects across the membranes. However,

when NMDG-aspartate was replaced by TMA-methanesulfonate (strong base/strong acid), the densities

of the acid (pH_o 4.5)-inducible inward currents were not significantly different from those recorded with

NMDG-aspartate (pH_p 6.5) (Fig. 4b).

The acid-inducible H^+-influx currents were observed in 4/10 undifferentiated, mononuclear RAW

cells cultured in the absence of sRANKL, and only in 1/10 wild COS7 cells (pH_o/pH_p 4.5/7.3). These

incidences were lower than those of osteoclasts. Consequently, the mean current-densities in RAW cells

and COS7 cells were significantly smaller than osteoclasts (Fig. 4c).

Effects of channel/transporter modulators on the acid-inducible H^+ influx currents

The effects of several widely-used channel/transporter modulators, which were reported to be

effective under pH_o as low as 4.5, on the acid-inducible inward currents were examined (Fig. 5a). Neither

DIDS (50 -100 μM), a non-specific blocker for anion channels/transporters, nor amiloride (100 μM), a

blocker for Na^+ channels (ENaC and ASIC channels) or Na^+-H^+ exchangers, affected the currents at 0 and

-80 mV. The current-densities of the H^+ influx activated in the presence of bafilomycin A_1 (200 nM), a

selective blocker for V-ATPases or DCCD (100-200 μM), a non-specific proton pump inhibitor, were not

significantly different from the controls.

Next, we examined the effects of divalent cations, calcium and zinc. There were no significant effects of $CaCl_2$ (10 mM) on the current densities (Fig.5a, rightmost). The acid-inducible inward currents were not affected by 0.2 mM $ZnCl_2$, but the current densities decreased slightly in the presence of 1 mM $ZnCl_2$ (Fig. 5b). When 1 mM $ZnCl_2$ was applied after the acid-inducible H^+ currents appeared, the currents were decreased (Fig. 5c, upper) without apparent changes in the slope ratio (lower). The inhibition by 1 mM $ZnCl_2$ was $14 \pm 10\%$ (n = 3) with pH_p 6.5 and $23 \pm 7\%$ (n = 5) with pH_p 7.3 (Fig. 5d). The inhibition seemed to be reversible, as removal of 1 mM $ZnCl_2$ increased the inward currents in 6 cells: the currents were recovered to $100 \pm 4\%$ of the amplitudes before additions of $ZnCl_2$.

Intracellular acidification induced by acid-inducible H^+ influx currents

In the whole-cell configuration, the interior of the cell is buffered with high concentrations of pH buffers in the pipette solutions. Still, the intracellular pH near the plasma membrane (pH_i) could be altered as a consequence of transmembrane H^+ fluxes [12, 19]. We estimated the changes in the pH_i during acid-exposures using the V_{rev}'s of voltage-gated H^+ channels (V_{rev-Hv}) (see methods) in cells exhibiting sufficient H^+ channel currents. The I-V relationships of the tail currents showed a shift of V_{rev-Hv}'s to more positive potentials by lowering pH_o (Fig. 6a-b). The mean V_{rev-Hv} values plotted against pH_o (Fig. 6c) deviated clearly from the E_H values calculated from the nominal ΔpH (pH_o - pH_p) (the dotted line) at low pH_o's (< 5.5). The pH_i's calculated as $pH_o + V_{rev-Hv} /58$ from the Nernst equation decreased steeply at < pH_o 5.5, for all pH_p's examined (Fig. 6d; triangles for pH_p 5.5, squares for pH_p 6.5 and circles for pH_p 7.3). The decreases in pH_i during acid exposures were supported by the findings that the H^+ channel currents showed an overshoot after removal of acids (Fig. 6e). During exposure to acids, the H^+ channel current amplitudes decreased and the V_{rev-Hv}'s, monitored continuously using current measurements at two voltages (see methods), shifted toward more positive voltages. Upon returning the pH_o to 7.3, the H^+ channel currents became larger and the V_{rev-Hv} values were lower than the controls

13

(arrows). The current amplitudes (80-100 mV for 0.5 s) were increased to more than 200% of the controls at the maximum after washing acids (pH_o 4.5) (Fig. 6f, left). The H^+ channel currents decreased gradually along the recovery of pH_i.

We examined the changes in the pH_i during acid-exposures in COS7 cells in which the acid-inducible inward H^+ currents were marginal. As wild type COS7 cells do not express native H^+ channels, the cells were transfected with a murine H^+ channel gene (Hv1/VSOP), which enabled us to evaluate the pH_i's in COS7 cells from the V_{rev-Hv}'s. The acid-inducible H^+ influx currents were hardly detected in the transformed COS7 (COS/Hv) cells, in none of 8 cells tested, under pH_o/pH_p 4.5/6.5. The decreases in pH_i in COS/Hv cells in the presence of extracellular acids (pH_o 4.5 and 5.5) were small (pH_p 6.5) (Fig. 6d, closed squares). The overshoots of the H^+ channel currents upon returning the pH_o from 4.5 to 7.3 were also small and transient in COS/Hv cells (Fig. 6f).

Whether the pH_i was affected by proton shuttle effects of NMDG-aspartate was also examined. At pH_o/pH_p 7.3/6.5, the pH_i estimated from the V_{rev-Hv} was 6.75 ± 0.05 (n = 42) in the presence of NMDG/aspartate and was 6.79 ± 0.04 (n = 15) when NMDG-aspartate were replaced by TMA-methanesulfonate. Exposure to acid (pH_o 4.5) decreased the pH_i to 5.41 ± 0.10 (n = 12) with NMDG-aspartate and to 5.37 ± 0.13 (n = 9) with TMA-methanesulfonate. Thus the pH_i's at pH_o 7.3 and pH_o 4.5 were not significantly different between the solutions containing NMDG-aspartate and TMA-methanesulfonate, suggesting that, under the present experimental conditions, proton-shuttle effects of NMDG/aspartate on the acid-induced pH_i changes were small if present at all.

Acid-inducible H^+ influx currents versus V-ATPase currents.

In the plasma membranes of osteoclasts, V-ATPases are essential to secrete protons into the extracellular space. We compared the current-densities of the acid-inducible H^+ influx currents (H^+-leak) with those of the H^+ efflux currents through the V-ATPases at different pH_o's (Fig. 7a). The V-ATPase

currents were identified as bafilomycin A_1 (200 nM)-sensitive currents [18]. V-ATPase currents were observed over a wide range of pH_o's (4.5 – 7.3) (open squares), while the H^+-leak currents were evident only at $pH_o < \sim 5.5$ (closed squares). Depolarizations increased V-ATPase currents and decreased the H^+-leak currents (-80 mV in left and 0 mV in right). The net H^+ currents, estimated from these H^+ fluxes in opposite directions, seemed to depend on pH_o's and voltages.

Discussion

Abundant H^+ efflux pathways are expressed in the plasma membrane of osteoclasts, such as V-ATPases, voltage-gated H^+ channels, and Na^+-H^+ exchangers. However, the H^+ influx pathways have not been investigated so far. In this study we provide evidence that exposure to strong extracellular acid ($< pH_o$ 5.5) activates an electrogenic H^+ influx pathway in the plasma membrane of RAW-derived osteoclasts. This acid-inducible H^+ influx is suggested to be a H^+-leak mechanism in the plasma membranes of osteoclasts upon exposure to highly acidified extracellular environments.

Properties of the acid-inducible H^+ influx currents. The acid-inducible inward currents were characterized by a slight inward rectification and by time-independent kinetics for activation and inactivation following hyperpolarization. The V_{rev}'s were dependent on the pH gradients across the membrane, and agreed well with the theoretical E_H values. The V_{rev} values were not dependent on the concentrations of other ions ($NMDG^+$, aspartate$^-$, Cl^-, Na^+ and HCO_3^-). The current amplitudes became larger after increasing the electrochemical driving force for the H^+ influx, but were not affected by changes in the concentrations of either Cl^-, Na^+ or HCO_3^-. Additionally, the intracellular pH was decreased by exposure to pH_o <5.5 which induced the inward currents. All these results suggest that the acid-inducible influx currents observed in the present recording conditions were largely mediated by protons.

Theoretically, it is difficult to distinguish between currents mediated by H^+ and OH^- in the opposite directions. The inward currents were increased by decreases in pH_o, which may be explained more easily by increases in the extracellular concentrations of H^+ rather than decreases in the extracellular concentrations of OH^-. Although we cannot rule out involvement of the proton equivalents, protons are the most likely candidate for mediating the influx currents at this moment.

The H^+ influx currents were not induced at $pH_o \geq 6.0$ for the pH_p's ranging from 5.5 to 7.3. At pH_o 5.5, the acid-inducible currents were present in ~20% of cells with pH_p 7.3 but were negligible with pH_p

16

5.5. The lower incidence at pH_p 5.5 might be partly due to an underestimation of the appearance because of the small amplitudes of the currents. At pH_o 4.5, the currents were present in ~90% of the cells with pH_p's ranging from 5.5 to 7.3. The activation threshold for the acid-inducible currents was thus likely to be $pH_o < ~5.5$.

Effects of channel/transporter inhibitors on the acid-inducible H^+ influx currents. At this moment, blockers for the acid-inducible H^+ influx currents remain unknown. Amiloride is known as a general blocker for Na^+ channels including ENaC and ASIC channels, and for Na^+-H^+ exchangers. The effectiveness of amiloride for ASIC channels under pH_o as low as 4.5 was reported [1, 11]. DIDS is a general blocker for anion channels/transporters and blocked the acid-sensitive Cl^- currents in osteoclasts almost completely at <50 mV at pH_o 4.5. The acid-inducible H^+ influx currents were not affected by amiloride and DIDS. We also examined the effects of extracellular divalent cations, Zn^{2+} and Ca^{2+}. Neither Ca^{2+} (up to 10 mM) nor 200 μM Zn^{2+} affected the acid-inducible H^+ influx currents. One mM Zn^{2+}, however, decreased the acid-inducible currents partially. Higher concentrations of these divalent cations have not been tested as they often activated Cl^- channels [21-22].

The proton fluxes through V-ATPases and the voltage-gated H^+ channels are generally one-directional, from inside to outside of the cells. Could reversed currents through these pathways mediate H^+ influxes during exposure to strong acids? This is an intriguing idea and might be worth investigation. The membrane sector of V-ATPases (V_o) has a passive proton conductance at pH 4.2, which is blocked by bafilomycin A_1 [3]. Proton shunts (reversed currents) at pH 3.0 have been reported in yeast V-ATPases [9]. However, in the present study, bafilomycin A_1 and DCCD, proton pump blockers, did not significantly inhibit the acid-inducible H^+ influx currents at pH_o 4.5. Also the voltage-gated H^+ channels did not seem to contribute to the acid-inducible H^+ influx currents, as the currents were not activated in COS7 cells expressing the H^+ channels. Thus both V-ATPases and voltage-gated H^+ channels are unlikely to mediate the acid-inducible H^+ influx currents described herein.

The molecular identity of the acid-inducible H^+ influx currents is presently unknown. The plasma membrane of osteoclasts express various acid-sensing cation channels (ASIC, TRP and HCN channels) [6, 8, 13, 16, 17] and acid-sensing anion channels (ClC7) [7]. However, these channels are unlikely to be responsible for the H^+ influx, as Na^+ and Cl^- did not affect the currents, although their contribution to the late currents remains to be resolved. Chang et al. [2] reported inward proton currents activated by strong acids (pH ~5) in sour taste cells. The currents are selective to protons, and are insensitive to bafilomycin A_1, amiloride and DIDS. Differently from the acid-inducible currents in osteoclasts described in this study, the currents in taste cells have higher sensitivity to Zn^{2+}: 1 mM Zn^{2+} blocks the currents nearly completely. They also do not display inward rectification. There are not sufficient data to compare these H^+ influx currents in more detail. It is intriguing, however, that these cells, which are exposed to strong acids, have the H^+ influx pathways.

Intracellular acidification by exposure to extracellular acids. We estimated the acid-induced changes in the pH_i in the vicinity of the plasma membrane from the V_{rev}'s of co-existing voltage-gated H^+ channels (V_{rev}-$_{Hv}$) [12, 19]. The pH_i was decreased steeply by exposure to $pH_o < 5.5$, near the threshold pH_o for activating the H^+ influx currents. The pH_i did not seem to be affected by the proton-shuttle with weak acid/base in solutions, as there were no significant differences between the acid-induced changes in pH_i in the presence of NMDG-aspartate (weak base/acid) and those in the presence of TMA-methanesulfonate (strong base/acid). In COS7 cells, in which acid-exposures hardly induced the acid-inducible H^+ influx currents, the pH_i decreases were small. These results suggested that the pH_i decreases in the vicinity of the plasma membrane exposed to $pH_o < 5.5$ were produced mainly by the acid-inducible H^+ influx currents.

It is noted that the voltage-gated H^+ channel currents were potentiated greatly upon removal of acids. The decreases in pH_i during acid exposures shifted the V_{rev}-$_{Hv}$'s to more negative potentials than the controls. The lowered pH_i was maintained for a while after the pH_o returned to the control level, which

increased the driving force for proton efflux through the H^+ channels. The overshoot of the H^+ channels was small and transient in COS7/Hv cells. The data suggested that the voltage-gated H^+ channels might contribute to reverse the intracellular acidification after the removal of extracellular acids in osteoclasts.

A consequence of the H^+ influx must be intracellular acidification. However, the measurements of pH_i's were made in the absence of major ions (Na^+, K^+, and Cl^-) which contribute to regulation of pH_i. Also there are limitations in estimating pH_i using the V_{rev}-$_{Hv}$'s: the values indicate the pH nearby the H^+ channels, but may not represent the mean pH_i of the whole cytosol. Although the H^+-influx currents could acidify osteoclasts, the net effects on pH_i's and osteoclast functions should be evaluated under more physiological conditions.

"H^+-leak" at the plasma membrane of osteoclasts. We started the present study, after being inspired by regulation mechanisms of intravesicular pH's of acidic vesicles. Intriguingly, the threshold pH_o for the acid-inducible H^+ influx currents is close to the vesicular pH of phagosomes or lysosomes ($<$ 5.5). The vesicular pH is considered to be regulated by balancing the H^+ accumulation by V-ATPases and H^+-leaks [4, 24, 26]. On the other hand, the H^+ fluxes in the plasma membranes of osteoclasts have been studied focusing on H^+ efflux mechanisms, that is, the proton pump (V-ATPases) activities of the plasma membrane. The present study provided evidence that the acid-inducible H^+ influx (H^+ leak) mechanism is also present in the plasma membrane. Along with extracellular acidification, the H^+ efflux through V-ATPases decreases and the H^+ influx increases. Amplitudes of both currents were also voltage-dependent: the pump currents were increased and the H^+ leak currents were decreased by depolarization. Thus the balance between the two currents varies according to ambient pH and voltages and also might be affected by the cellular conditions in individual cells. Importantly, the working range of pH_o was wide for the V-ATPase currents but was limited ($pH_o < 5.5$) for the H^+ leak currents.

Hydroxyapatite, a major component of bone minerals, was dissolved by a 3 min-exposure to pH 5.5 only slightly (~5%) (Fig. 7b, left). The dissolution at pH 5.5, however, became significant when the

exposure period was prolonged (right) (~30% for 3 h). The pH in the resorption pit is reported to be ranged from 4.7 – 6.8 [23]. It is suggested that protons secreted by V-ATPases acidify the pit and then the H^+-leak pathway will be activated when the pH_o is decreased sufficiently (Fig. 7c): the resultant pH_o depends on the amounts of these H^+ fluxes in opposite directions. It is conceivable that the two-way H^+ flux mechanisms, which are pumping out of protons by V-ATPases and uptake of protons by the H^+-leak pathway, may have advantages in fine regulation of ambient pH. It remains to be clarified whether the H^+-leak pathway is also expressed in the ATPase-rich membranes of acidic vesicles or not. Identification of the molecular mechanism behind the acid-inducible H^+ currents would advance our understanding of the physiological/pathological relevance of the novel H^+-leak pathway to cellular functions.

References

1. Askwith CC, Wemmie JA, Price MP, Rokhlina T, Welsh MJ (2004) Acid-sensing ion channel 2 (ASIC2) modulates ASIC1 H$^+$-activated currents in hippocampal neurons. J Biol Chem 279:18296-18305.   PMID 14960591

2. Chang RB, Waters H, Liman ER (2010) A proton current drives action potentials in genetically identified sour taste cells. Proc Natl Acad Sci USA 107: 22320-22325.   Doi: 10.1073/pnas.1013664107.

3. Crider BP, Xie X-S, Stone DK (1994) Bafilomycin inhibit proton flow through the H$^+$ channel of vacuolar proton pump. J Biol Chem 269:17379-17381.   PMID 8021236.

4. Grabe M, Oster G (2001) Regulation of organelle acidity. J Gen Physiol 117:329-343.   PMID 11279253.

5. Humez S, Fournier F, Guilbault P (1995) A voltage-dependent and pH-sensitive proton current in *Rana esculenta* oocytes. J Memb Biol 147:207-215.   PMID 8568856.

6. Jahr H, van Driel M, van Osch GJVM, Weinans H, van Leeuwen JPTM (2005) Identification of acid-sensing ion channels in bone. Biochem Biophys Res Comm 337:349-354. doi:10.1016/j.bbrc.2005.09.054

7. Kajiya H, Okamaoto F, Ohgi K, Nakao A, Fukushima H, Okabe K (2009) Characteristics of ClC7 Cl$^-$ channels and their inhibition in mutant (G215R) associated with autosomal dominant osteopetrosis type II in native osteoclasts and hClcn7 gene-expressing cells. Pflügers Arch 458:1049-1059. Doi: 10.1007/s00424-009-0689-4.

8. Kato K, Morita I (2013). Promotion of osteoclast differentiation and activation in spite of impeded osteoclast-lineage differentiation under acidosis: effects of acidosis on bone metabolism. BioSci Trends 7:33-41.   Doi: 10.5582/bst.2013.v7.1.33

9. Kettner C, Bertl A, Obermeyer G, Slayman C, Bihler H (2003) Electrophysiological analysis of the

yeast V-type proton pump: variable coupling ratio and proton shunt. Biophys J 85:3730-3738. PMID 14645064.

10. Kuno M, Ando H, Morihata H, Sakai H, Mori H, Sawada M, Oiki S (2009) Temperature dependence of proton permeation through a voltage-gated proton channel. J Gen Physiol 134:191-205. Doi: 10.1085/jgp.200910213.

11. Lingueglia E (2007) Acid-sensing ion channels in sensory perception. J Biol Chem 282:17325-17329. PMID 17430882.

12. Matsuura T, Mori T, Hasaka M, Kuno M, Kawawaki J, Nishikawa K, Narahashi T, Sawada M, Asada A (2012) Inhibition of voltage-gated proton channels by local anaesthetics in GMI-R1 rat microglia. J Physiol 590:827-843.　Doi: 10.1113/jphysiol.2011.218149.

13. Mizoguchi F, Mizuno A, Hayata T, Nakashima K, Heller S, Ushida T, Sokabe M, Miyasaka N, Suzuki M, Ezura Y, Noda M (2008) Transient receptor potential vanilloid 4 deficiency suppresses unloading-induced bone loss. J Cell Physiol 216:47-53.　PMID 18264976

14. Mori H, Sakai H, Morihata H, Kawawaki J, Amano H, Yamano T, Kuno M (2003) Regulatory mechanisms and physiological relevance of a voltage-gated H^+ channel in murine osteoclasts: phorbol myristate acetate induced cell acidosis and the channel activation. J Bone Miner Res 18:2069-2076.　PMID 14606521.

15. Nordström T, Rotstein OD, Romanek R, Asotra S, Heersche JNM, Manolson MF, Brisseau GF, Grinstein S (1995) Regulation of cytoplasmic pH in osteoclasts. Contribution of proton pumps and a proton-selective conductance. J Biol Chem 270:2203-2212.　PMID 7836451.

16. Notomi T, Kuno M, Ohura K, Noda M, Skerry TM (2015) Zinc-induced effects on osteoclastogenesis involve activation of hyperpolarization-activated cyclic nucleotide modulated channels via changes in membrane potential. J Bone Miner Res 30: 1618- 1626.　Doi: 10.1002/jbmr.2507.

17. Rossi F, Siniscalco D, Luongo L, De Petrocellis L, Bellini G, Petrosino S, Torella M, Santoro C,

Nobili B, Perrotta S, DiMazro V, Maione S (2009) The endovanilloid/endocannabinoid system in human osteoclasts: possible involvement in bone formation and resorption. Bone 44:476–84. PMID: 19059369.

18. Sakai H, Kawawaki J, Moriura Y, Mori H, Morihata H, Kuno M (2006) pH dependence and inhibition by extracellular calcium of proton currents via plasmalemmal vacuolar-type H^+-ATPase in murine osteoclasts. J Physiol 576:417-425.   Doi:10.1113/physiol.2006.117176.

19. Sakai H, Li G, Hino Y, Moriura Y, Kawawaki J, Sawada M, Kuno M (2013) Increases in intracellular pH facilitate endocytosis and decrease availability of voltage-gated proton channels in osteoclasts and microglia. J Physiol 591:5851-5866.   Doi: 10.1113/jphysiol.2013.263558.

20. Sakai H, Moriura Y, Notomi T, Kawawaki J, Ohnishi K, Kuno M (2010) Phospholipase C-dependent Ca^{2+}-sensing pathways leading to endocytosis and inhibition of the plasma membrane vacuolar H^+-ATPase in osteoclasts. Am J Physiol (Cell Physiol) 299:C570-C578.   Doi: 10.1152/ajpcell.00486.2009.

21. Sakai H, Nakamura F, Kuno M (1999) Synergetic activation of outwardly rectifying Cl^- currents by hypotonic stress and external Ca^{2+} in murine osteoclasts. J Physiol 515:157-168.   PMID 9925886.

22. Sakuta K, Sakai H, Mori H, Morihata H, Kuno M (2002) Na^+ dependence of extracellular Ca^{2+}-sensing mechanisms leading to activation of an outwardly rectifying Cl^- channel in murine osteoclasts. Bone 31:374-380.   PMID 12231409.

23. Silver IA, Murrills RJ, Etherington DJ (1988) Microelectrode studies on the acid microenvironment beneath adherent macrophages and osteoclasts. Exp Cell Res 175:266-276.   PMID 3360056.

24. Steinberg BE, Touret N, Vargas-Caballero M, Grinstein S (2007) In situ measurement of the electrical potential across the phagosomal membrane using FRET and its contribution to the proton-motive force. Proc Natl Acad Sci USA 104:9523-9528.   Doi: 10.1073/pnas.0700783104.

25. Toyomura T, Murata Y, Yamamoto A, Oka T, Sun-Wada GH, Wada Y, Futai M (2003) From

lysosomes to the plasma membrane: localization of vacuolar-type H^+-ATPase with the a3 isoform during osteoclast differentiation. J Biol Chem 278:22023-22030.　PMID 12672822.

26. Van Dyke RW (1993) Acidification of rat liver lysosomes: quantitation and comparison with endosomes. Am J Physiol 265:C901-C917. PMID 823831.

Fig. 1 Acid-induced changes in H$^+$ currents

Fig. 1
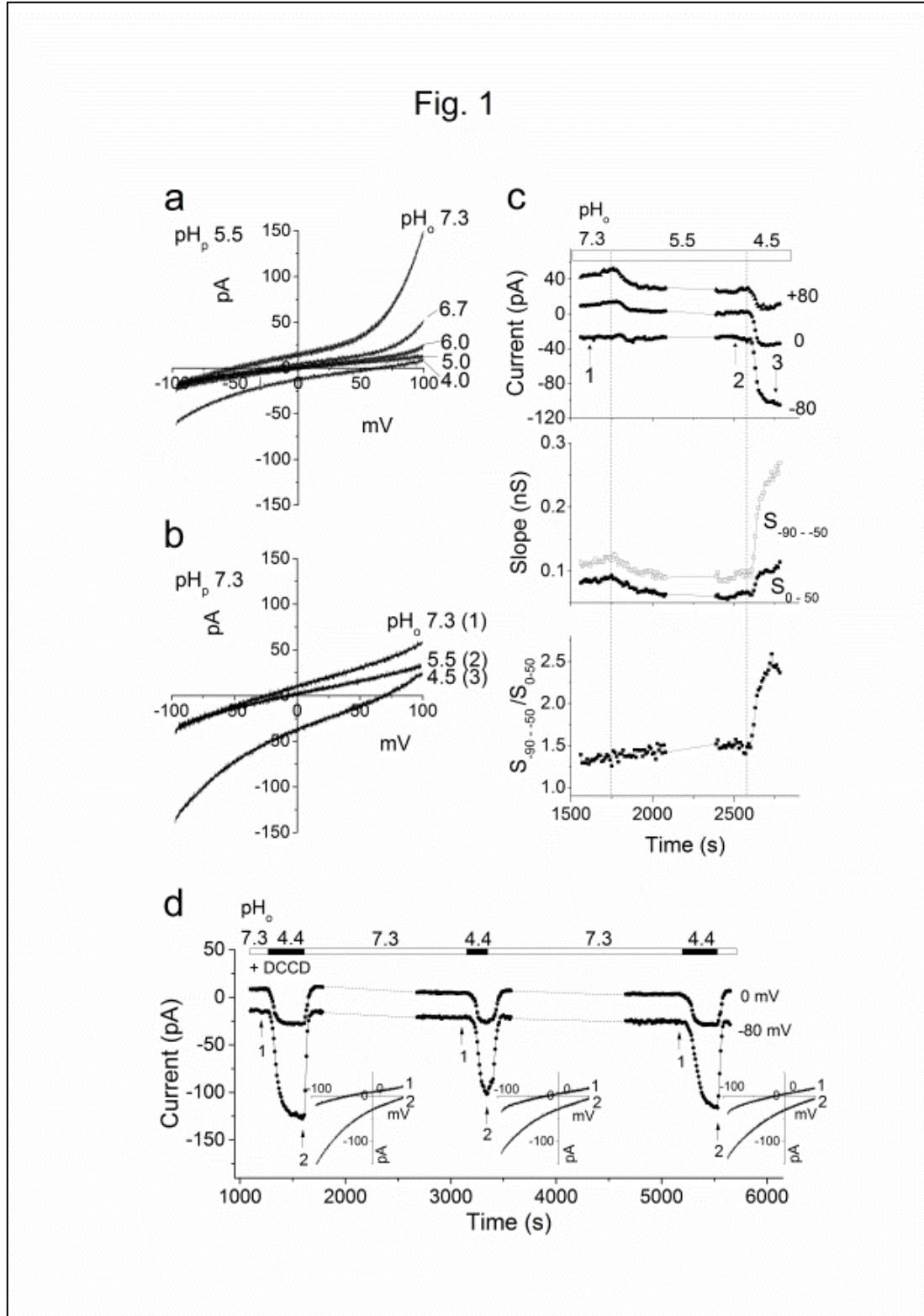
a, I-V relationships of whole-cell H^+ currents evoked by voltage ramps applied at a holding potential of -80 mV. The pH_o was lowered stepwise from 7.3, to 6.7, 6.0, 5.0 and 4.0. The pH_p was 5.5. **b,** I-V relationships for the currents in a cell exposed to pH_o 7.3, 5.5 and 4.5. The pH_p was 7.3. **c,** time courses of the acid inducible currents at three potentials (-80, 0 and +80 mV) (top), slopes of the I-V relationships over -90 - -50 mV (open squares, $S_{-90--50}$) and 0 – 50 mV (closed squares, S_{0-50}) (middle), and the slope ratio ($S_{-90--50}/ S_{0-50}$) (bottom). The data from b and c were obtained from the same cell. The current traces in 1-3 in b were recorded at time 1-3 indicated in c. The abscissa represents time after the whole-cell configuration was made. **d,** the time courses of the changes in the current amplitudes (0 and -80 mV) in the presence of 200 μM DCCD, a proton pump inhibitor. The pH_o was lowered from 7.3 to 4.4 repeatedly: the exposure periods were 6, 3 and 5 min for each. The inset records represent the I-V relationships obtained at time-1 and -2 during each trial. The pH_p was 7.0.

Fig. 2 Effects of acids on the whole-cell currents


Fig.2
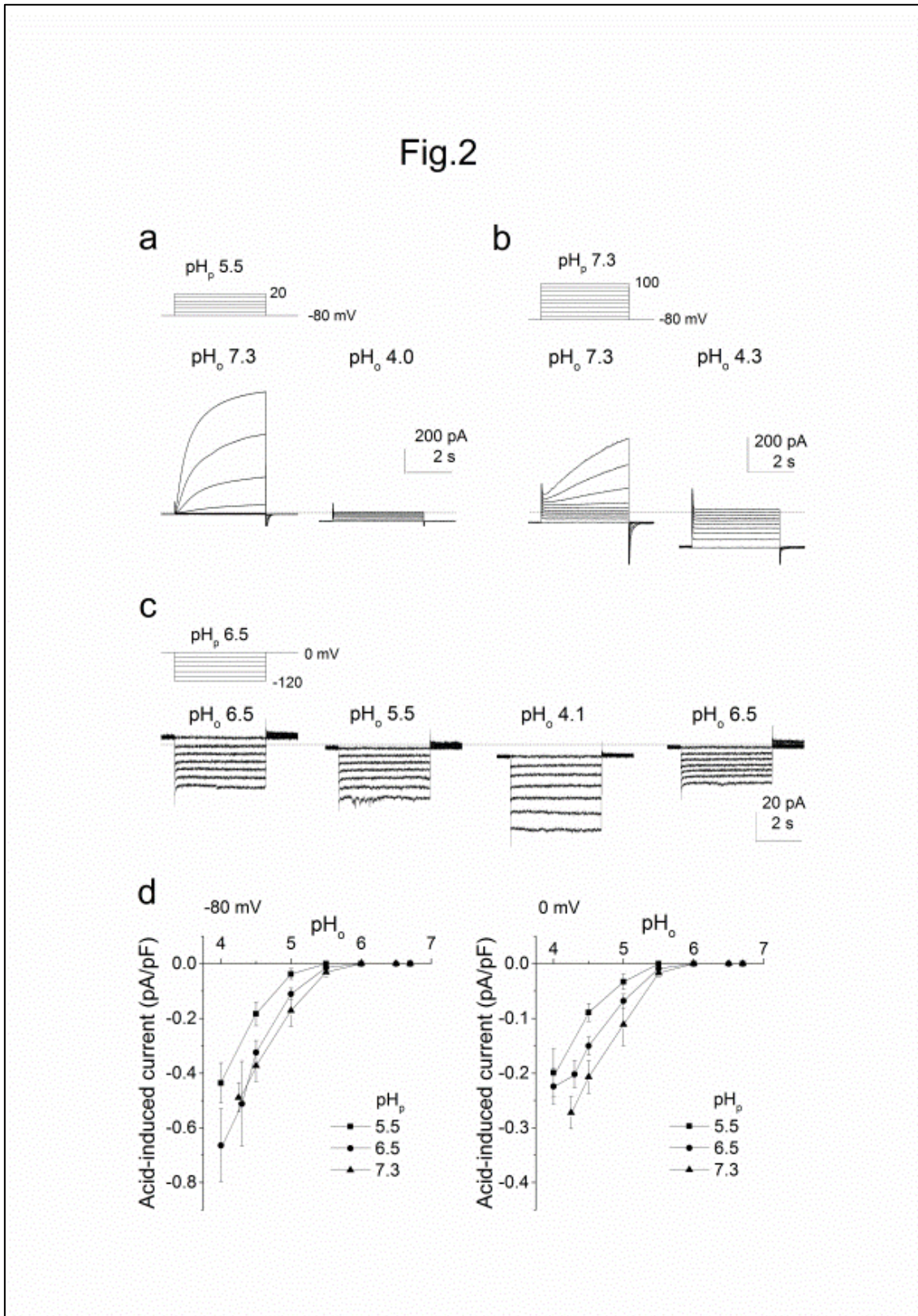
a-b, whole cell currents evoked by depolarization pulses applied at a holding potential of -80 mV with pH$_p$ 5.5 (a) and 7.3 (b). The pH$_o$ was decreased from 7.3 to 4.0 in a and, to 4.3 in b. **c,** whole cell currents evoked by hyperpolarization pulses applied at a holding potential of 0 mV (pH$_p$ 6.5). The pH$_o$ was decreased from 6.5 to 5.5 and 4.1, and then returned to 6.5. The dotted line indicates the zero current level. **d,** the densities of the acid-inducible currents under different pH$_p$'s (5.5, 6.5 and 7.3). The data at -80 mV (left) and 0 mV (right) are plotted against pH$_o$ (n = 8 - 23). Data are means ± sem.

**Fig. 3 The reversal potentials for the acid-inducible inward currents**
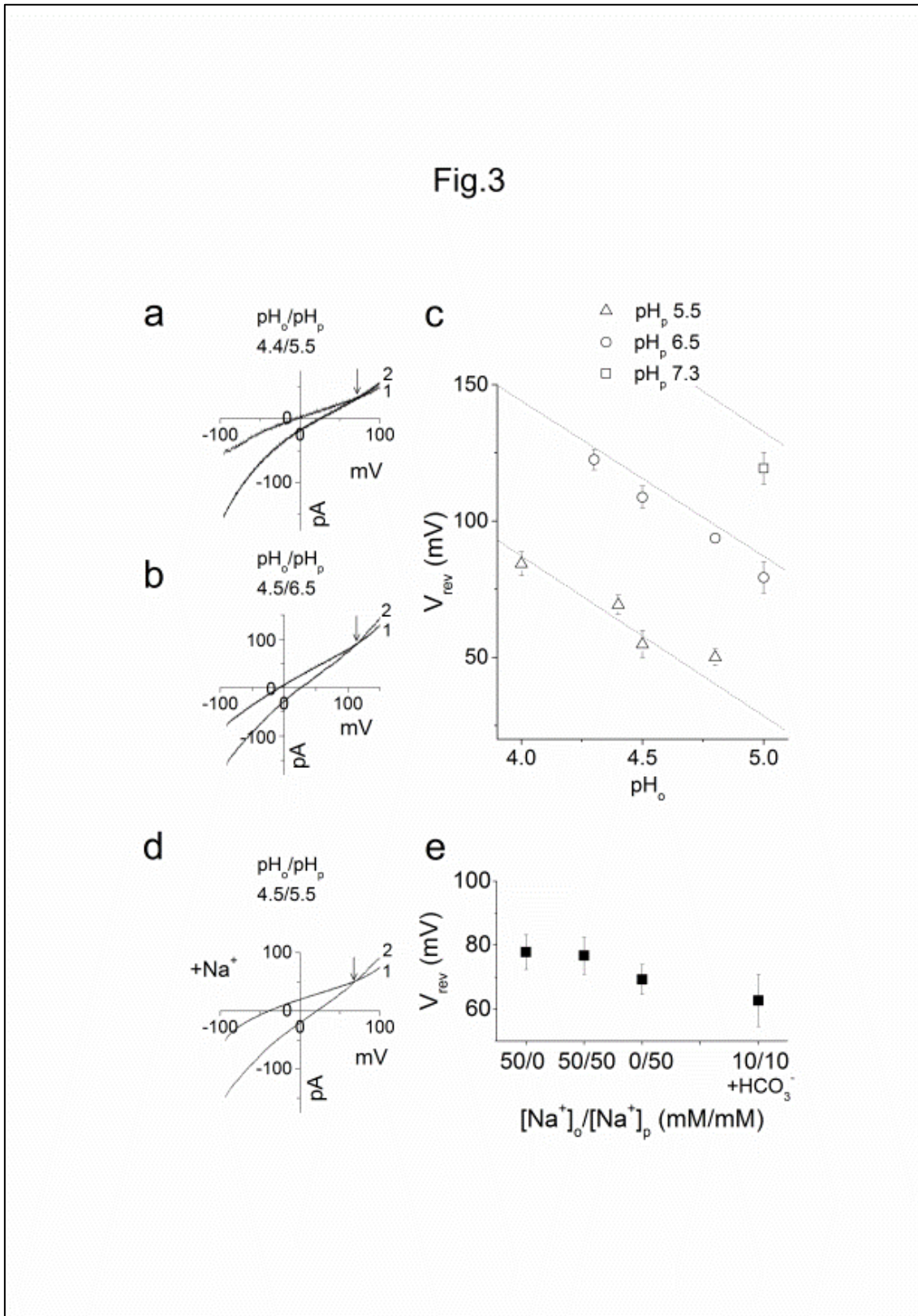
a-b, the I-V relationships before (1) and after (2) activation of the acid-induced inward currents (pH_o/pH_p

4.4/5.5 in a and 4.5/6.5 in b). Each trace is average of 2-5 recordings. The background currents were not

subtracted. The voltage ramps up to 100 mV (a) or 150 mV (b) were applied at the holding potential (-80

mV). Arrows indicate the reversal potentials (V_{rev}), 73 mV for a and 114 mV for b. **c,** the $V_{rev} - pH_o$ plots

of the acid-inducible inward currents (triangles for pH_p 5.5, circles for pH_p 6.5 and squares for pH_p 7.3) (n

= 3 - 21). The dotted lines indicate equilibrium potentials of H^+ for the different pH_p's. **d,** the I-V

relationships recorded before (1) and after (2) activation of the acid-inducible currents in the presence of

Na^+ (pH_o/pH_p 4.5/5.5). Both bath and pipette solutions contained 50 mM Na^+. The V_{rev} was 70 mV

(arrow). **e,** the V_{rev}'s of acid-inducible currents (pH_o/pH_p 4.5/5.5) for different transmembrane

concentration gradients of Na^+ (n = 3 - 5). The right most represents the V_{rev}'s in the presence of 10 mM

$NaHCO_3$ in both bath and pipette solutions (n = 3). There was no significant difference in the V_{rev}'s. In c

and e, data are means ± sem.

Fig. 4 Effects of ions on the amplitudes of the acid -inducible H$^+$ influx currents
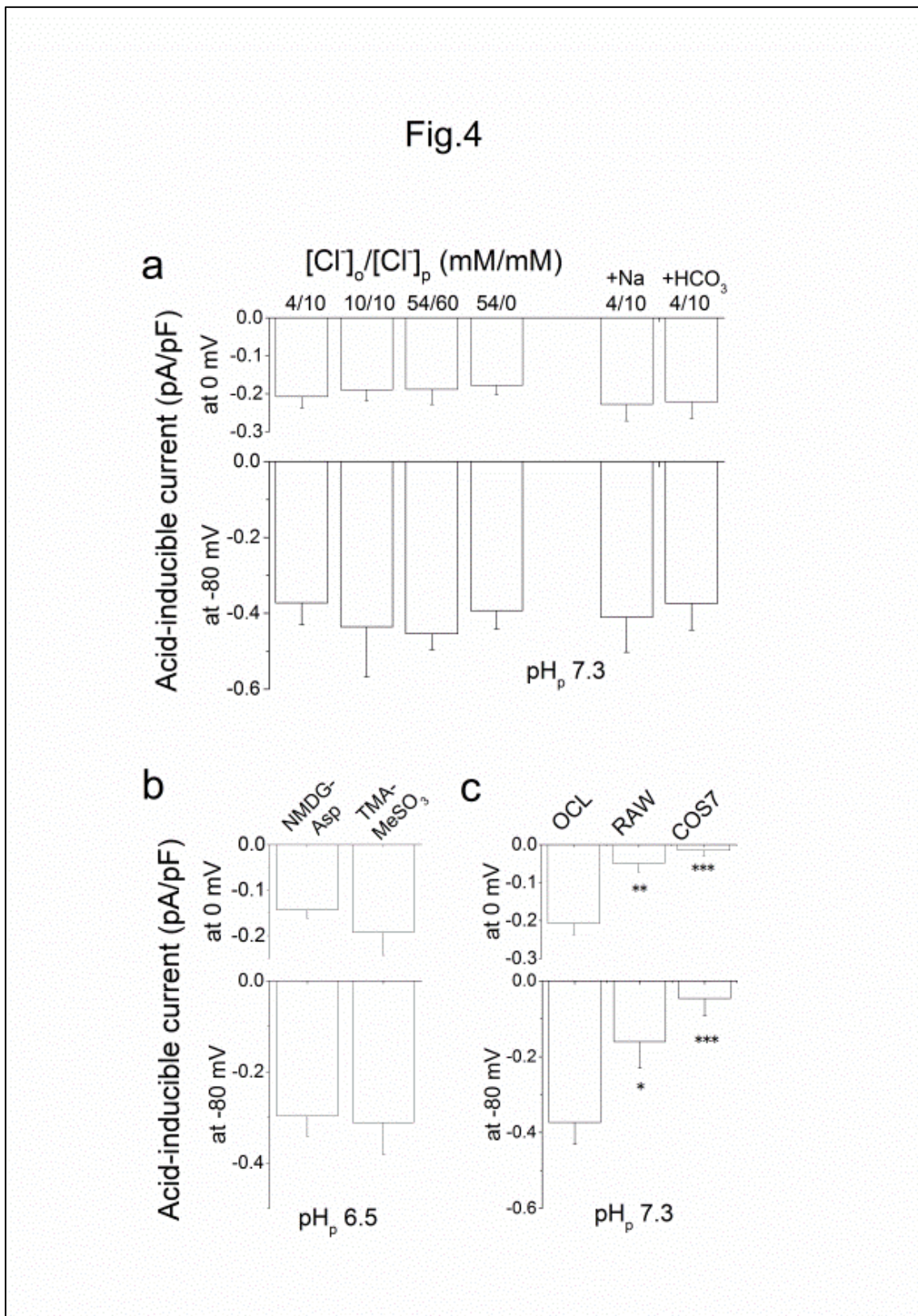
a, the current-densities at 0 and -80 mV, in the presence of different combinations of extracellular and intracellular Cl$^-$ concentrations ([Cl]$_o$/[Cl]$_p$) (in mM) (n = 4 - 19). In the right columns, 50 mM Na$^+$ or 10 mM NaHCO$_3$ was present in both extracellular and intracellular solutions (n = 5). **b,** the current-densities at 0 and -80 mV when NMDG-aspartate was replaced by TMA-methanesulfonate (TMA-MeSO$_3$). **c,** the current-densities in osteoclasts (n = 19), undifferentiated mononuclear RAW cells (n = 10) and in wild-type COS7 cells (n = 10). *p < 0.05, ** p < 0.005 and ***p <0.001, compared with osteoclasts. In a-c, all solutions contained 50 – 100 μM DIDS and the pH$_o$ was 4.5. The pH$_p$ was 7.3 for a and c, and 6.5 for b. Data are means ± sem.

**Fig. 5 Effects of channel/transporter blockers on the acid-inducible H$^+$ currents**
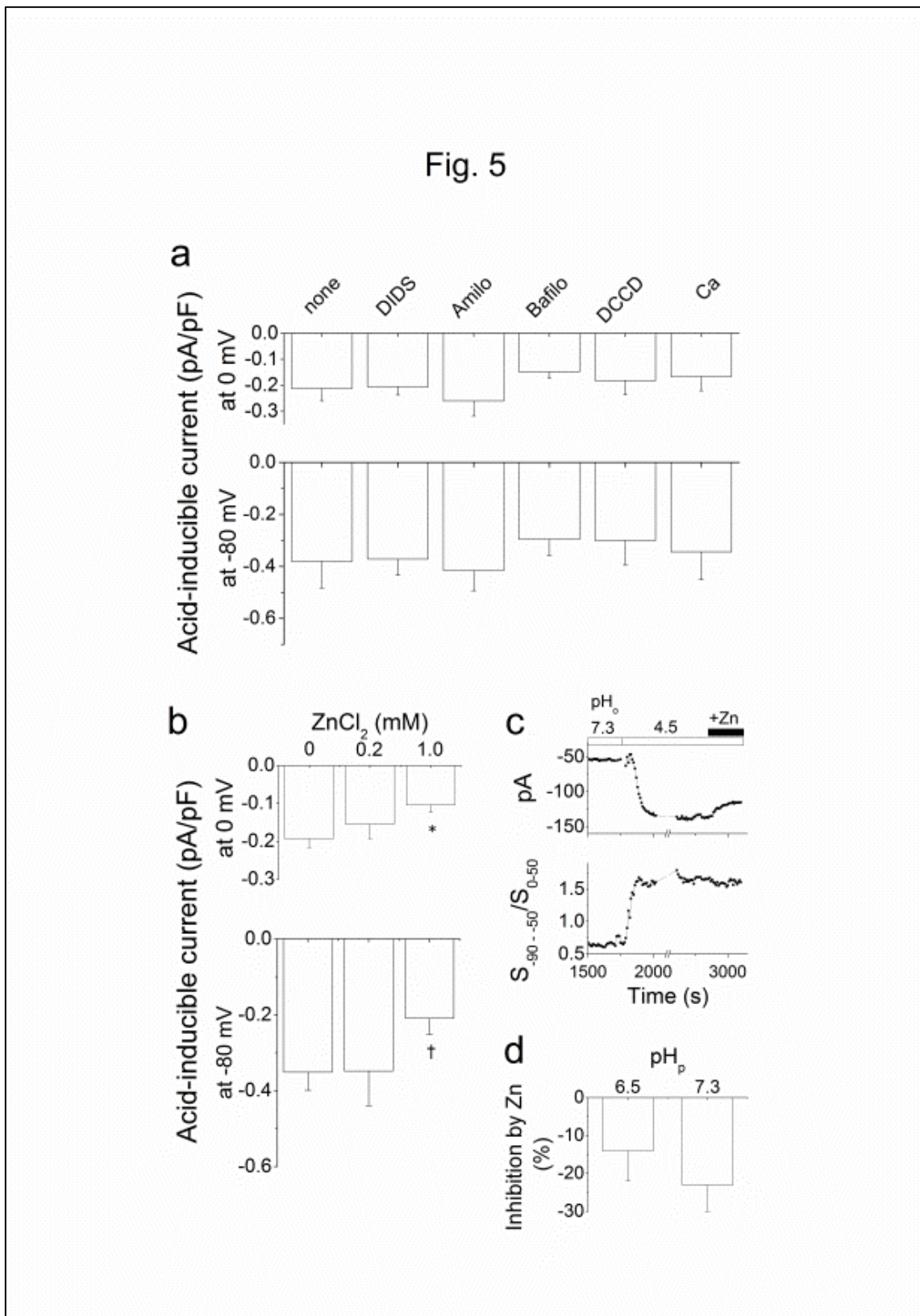
a, the current-densities of the acid (pH_o 4.5)-inducible H^+ currents at 0 and -80 mV under pH_p 7.3, in the absence of blockers (none, n = 6), in the presence of 50-100 μM DIDS (n = 18), 100 μM amiloride (n = 8), 200 nM bafilomycin A_1 (n = 11), 100 μM DCCD (n = 6) and 10 mM $CaCl_2$ (n = 4). **b,** the current-densities of the acid-inducible H^+ currents (pH_o/pH_p 4.5/7.3) activated in the presence of 0, 0.2 and 1.0 mM $ZnCl_2$ (n = 12-17). All extracellular solutions contained 100 μM DIDS. *p < 0.05. †p = 0.06. **c,** the time courses of the changes in the current amplitudes at -80 mV (upper) and the slope ratios of the I-V relationships (lower) of the acid-inducible H^+ currents (pH_o/pH_p 4.5/6.5). $ZnCl_2$ (1 mM) was added after the acid-inducible currents reached the steady-state. **d,** the inhibition of the acid (pH_o 4.5)-inducible currents (-80 mV) by 1 mM $ZnCl_2.$ pH_p's were 6.5 or 7.3 (n = 3-5). Data are means ± sem.

Fig. 6 Extracellular acid-induced intracellular acidification

Fig. 6
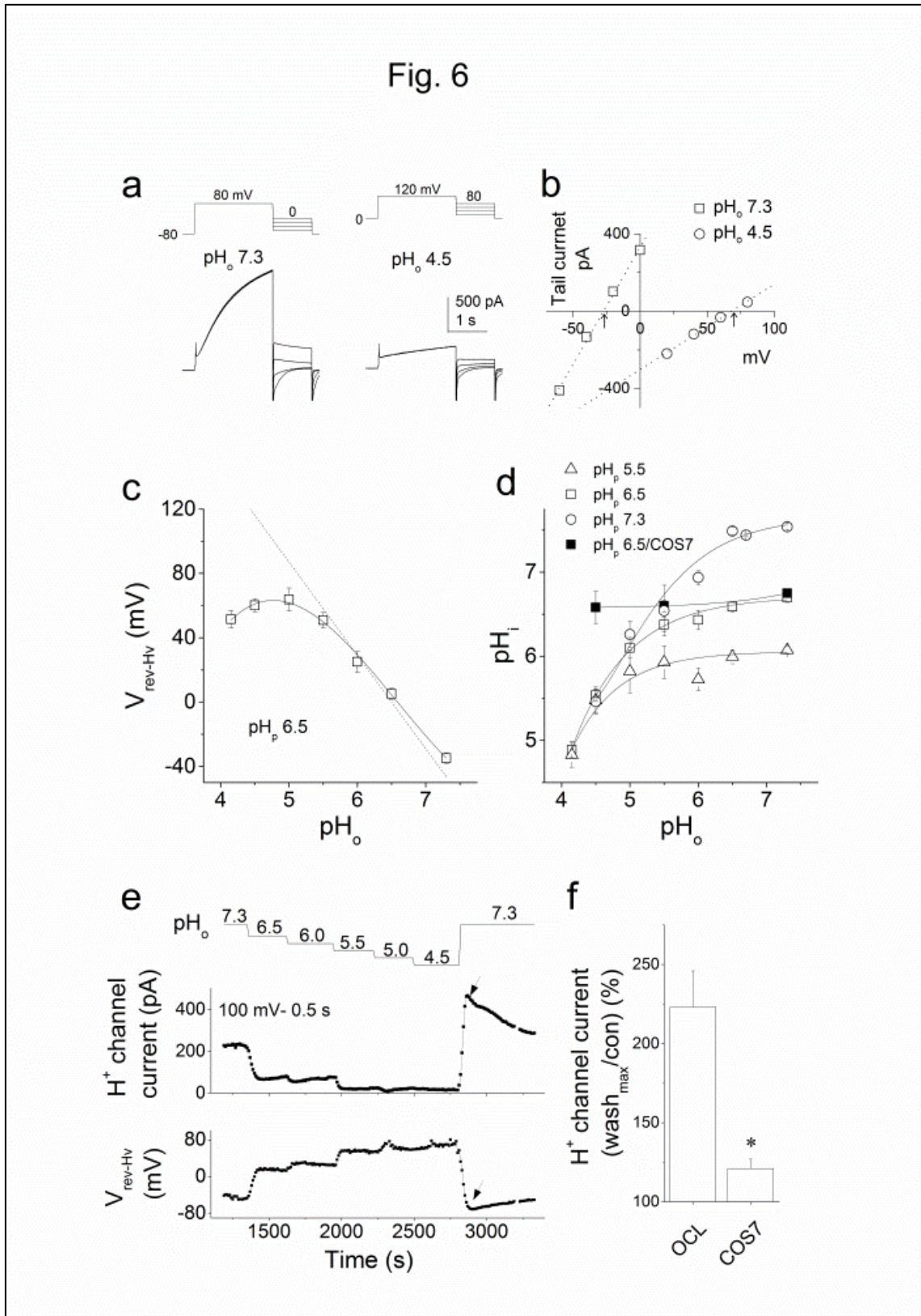
a-b, estimation of the reversal potentials for the H^+ channel (V_{rev-Hv}) with the tail current method. Tail currents were recorded at different voltages following 1 s-long prepotentials (80 mV for pH_o 7.3 and 120 mV for pH_o 4.5) (a). After subtraction of leak currents at each voltages, the net tail currents were plotted against the voltages (b). The V_{rev-Hv}'s were indicated by arrows. The pH_p was 6.5. **c,** a plot of the V_{rev-Hv} values against the pH_o (n = 3 - 25). The dotted line indicates the E_H estimated from the pH_o and pH_p (6.5). **d,** the intracellular pH (pH_i) calculated from the V_{rev-Hv} values using the Nernst equation at each pH_o. pH_p's were 5.5 (triangles, n = 2 - 42), 6.5 (squares, n = 3 − 25) and 7.3 (circles, 2 − 42). The pH_i in COS7 cells transfected with a H^+ channel gene were indicated by closed squares (pH_p 6.5) (n = 5 − 10). **e,** the changes in the H^+ channel current amplitudes (middle) and the V_{rev-Hv}'s (bottom) in an osteoclast (pH_p 6.5). The pH_o was decreased stepwise, from 7.3 to 4.5, and then was returned to 7.3. The current-amplitudes (upper) were measured at the end of the depolarization pulses (100 mV − 0.5 s) applied at a holding potential (-40 mV) and the V_{rev-Hv} (lower) were estimated from the current amplitudes at two voltages, either 100 and 40 mV or 40 and -40 mV. **f,** overshoot of the H^+ channel currents after removal of acid (pH_o 4.5) in osteoclasts and COS7 cells transfected with a H^+ channel gene. The currents (100 or 80 mV for 0.5 s) were measured under pH_o/pH_p 7.3/6.5. The maximal current-densities after washing acids were expressed as percent of the controls. In c, d and f, data are means ± sem.

Fig. 7 V-ATPase currents versus H$^+$-leak currents

Fig. 7
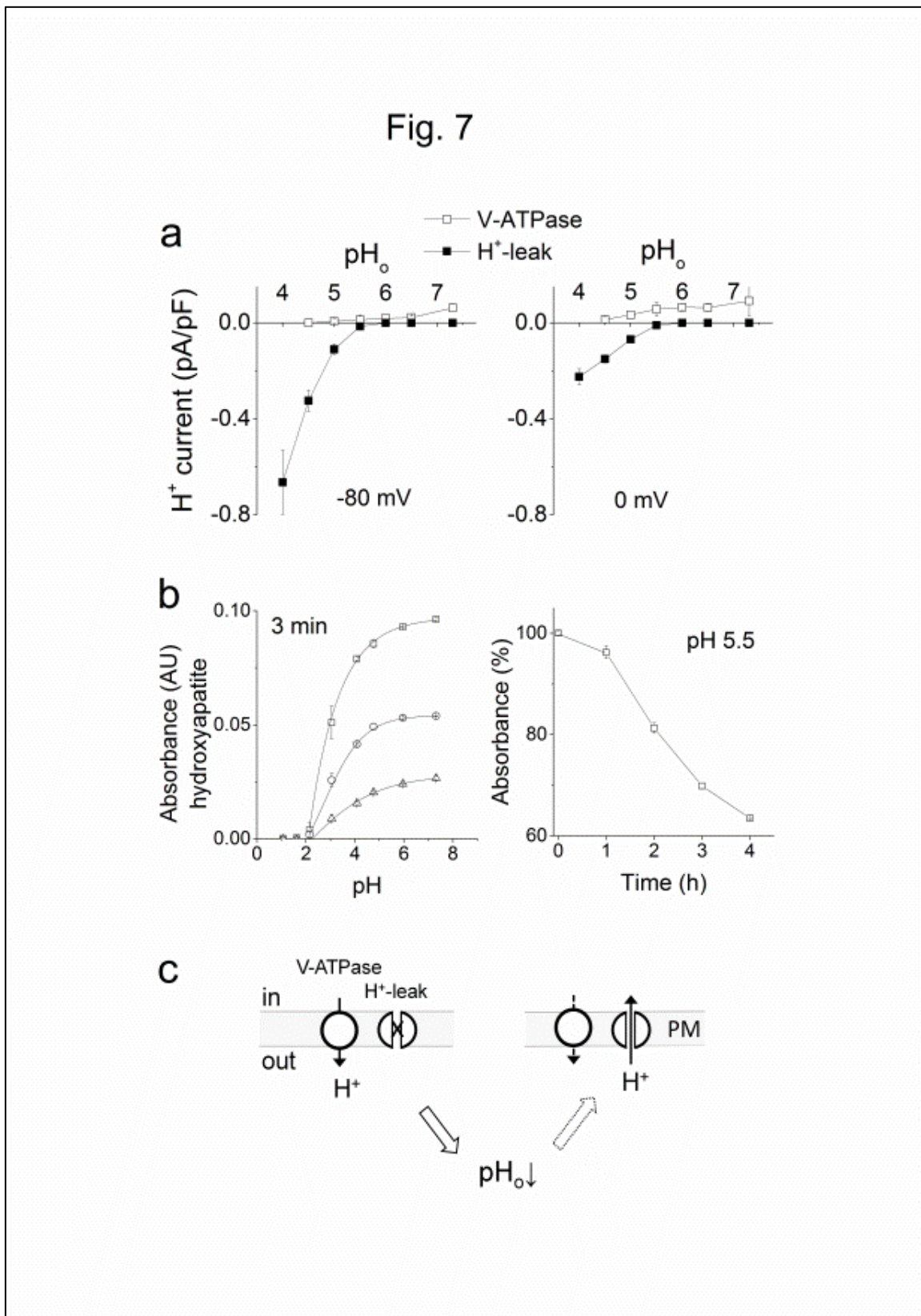
a, current-densities of outward H^+ currents through V-ATPases (open squares; n = 3-19) and the acid-inducible inward H^+ currents (closed squares; n = 9-21) recorded at -80 mV (left) and 0 mV (right). The pH_p was set at 6.5. V-ATPase currents were identified as bafilomycin-sensitive currents. **b,** dissolution of hydroxyapatites by acids. Left, absorbance of the Ringer solutions containing hydroxyapatite particles exposed to different pHs for 3 min (n = 3) (in arbitrary units, AU). The suspensions contained hydoxypatate at 0.1 (triangles), 0.25 (circles) and 0.5 (squares) mg/ml. Right, the time course of dissolution of hydroxyapatite (0.5 mg/ml) at pH 5.5 (n = 3). **c,** a simplistic cartoon of the proton fluxes at the plasma membrane of osteoclasts. The plasma membranes are rich in proton pumps, vacuolar H^+-ATPases. Protons are secreted by V-ATPase, and then acidify the extracellular space. When the pH_o is sufficiently decreased, the proton extrusion decreases and the H^+-leak (acid-inducible H^+ influx) pathway will be activated. In a and b, data are means ± sem.